

Liquiritigenin-Loaded Submicron Emulsion Protects Against Doxorubicin-Induced Cardiotoxicity via Antioxidant, Anti-Inflammatory, and Anti-Apoptotic Activity

This article was published in the following Dove Press journal:
International Journal of Nanomedicine

Changcan Shi^{1,*}
Hongjuan Wu^{2,*}
Ke Xu³
Ting Cai³
Kunming Qin⁴
Li Wu¹
Baochang Cai^{1,4}

¹School of Pharmacy, Nanjing University of Chinese Medicine, Nanjing 210046, People's Republic of China; ²Nanjing Jiangning District Hospital of Traditional Chinese Medicine, Nanjing 211100, People's Republic of China; ³School of Pharmacy, China Pharmaceutical University, Nanjing 210009, People's Republic of China; ⁴Nanjing Haichang Chinese Medicine Group Corporation, Nanjing 210061, People's Republic of China

*These authors contributed equally to this work

Background: The clinical use of doxorubicin (DOX) is severely limited due to its cardiotoxicity. Thus, there is a need for prophylactic and treatment strategies against DOX-induced cardiotoxicity.

Purpose: The purpose of this study was to develop a liquiritigenin-loaded submicron emulsion (Lq-SE) with enhanced oral bioavailability and to explore its efficacy against DOX-induced cardiotoxicity.

Methods: Lq-SE was prepared using high-pressure homogenization and characterized using several analytical techniques. The formulation was optimized by central composite design response surface methodology (CCD-RSM). In vivo pharmacokinetic studies, biochemical analyses, reactive oxygen species (ROS) assays, histopathologic assays, and Western blot analyses were performed.

Results: Each Lq-SE droplet had a mean particle size of 221.7 ± 5.80 nm, a polydispersity index (PDI) of 0.106 ± 0.068 and a zeta potential of -28.23 ± 0.42 mV. The area under the curve (AUC) of Lq-SE was 595% higher than that of liquiritigenin (Lq). Lq-SE decreased the release of serum cardiac enzymes and ameliorated histopathological changes in the hearts of DOX-challenged mice. Lq-SE significantly reduced oxidative stress by adjusting the levels of ROS, increasing the activity of antioxidative enzymes and inhibiting the protein expression of NOX4 and NOX2. Furthermore, Lq-SE significantly improved the inflammatory response through the mitogen-activated protein kinase (MAPK)/nuclear factor- κ B (NF- κ B) signalling pathway and induced cardiomyocyte apoptosis.

Conclusion: Lq-SE could be used as an effective cardioprotective agent against DOX in chemotherapy to enable better treatment outcomes.

Keywords: liquiritigenin, submicron emulsion, bioavailability, cardiotoxicity, protective efficacy

Correspondence: Li Wu
School of Pharmacy, Nanjing University of Chinese Medicine, Nanjing 210046, People's Republic of China
Email wuli@njucm.edu.cn

Baochang Cai
School of Pharmacy Nanjing University of Chinese Medicine, Nanjing 210046, People's Republic of China
Email bccai@126.com

Introduction

Doxorubicin (DOX), an anthracycline antibiotic, has been the most widely used effective anticancer agent for the treatment of various human cancers, including both haematologic malignancies and solid tumours, for 50 years.^{1,2} Nevertheless, the clinical utility of DOX is limited due to its marked cardiotoxicity.^{3,4} DOX-induced cardiotoxicity mainly involves myocardial enzyme abnormalities, cardiomyocyte damage, and apoptotic and necrotic cell death.⁵ The molecular mechanisms through which DOX induces

cardiotoxicity remain ambiguous. However, the major cellular processes involved include oxidative stress, the inflammatory response, mitochondrial dysfunction, calcium dysregulation, autophagy, and cell death.^{6–8} Oxidative stress is one of the major effects of DOX-induced cardiotoxicity, and reactive oxygen species (ROS) play crucial roles in this process. Some studies have shown that inhibition of oxidative stress can prevent DOX-induced cardiotoxicity.^{9,10} Currently, increasing research is being conducted on prophylactic and treatment measures for DOX-induced cardiotoxicity.^{11–14}

Traditional Chinese medicines are widely used as adjuvants in the treatment of cancer because they often exert synergistic effects and reduce adverse reactions to chemotherapy agents.^{15–17} Liquiritigenin (Lq) (Figure 1) is a type of flavonoid derived from *Glycyrrhiza glabra* (GG). GG has been widely used in Chinese herbal medicine for thousands of years. In previous studies, Lq has been reported to exert various biochemical effects, including oxidative stress inhibition and anti-inflammatory, anti-allergic, anti-hyperlipidaemic, hepatoprotective, and proapoptotic effects.^{18–21} Lq shows the stronger radical scavenging capacity than isobavachin and was in the same range as apigenin in the DPPH assay.²² Lq has been shown to inhibit the growth of human cervical carcinoma (HeLa) cells and to induce apoptosis in human hepatoma SMMC-7721 cells.^{23,24} Lq also has cytoprotective effects against heavy metal-induced toxicity in cultured cells.²⁵ Additionally, treatment with Lq improves high fructose feeding-induced cardiac injury by inhibiting the progression of fibrosis and the inflammatory response through mediation of the NF- κ B signalling pathway.²⁶ Therefore, in this study, the protective effects of Lq for the prevention and treatment of DOX-induced cardiotoxicity and the underlying mechanisms of these effects were evaluated. Notably, application of Lq has been limited by its low aqueous and lipid solubility,²⁷ which markedly reduce the efficacy of Lq. Therefore, it is necessary

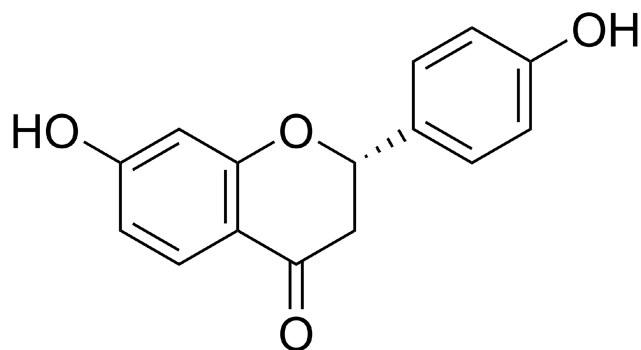


Figure 1 Chemical structure of liquiritigenin.

to develop a novel drug delivery system to improve the bioavailability and efficacy of Lq.

Oral delivery systems are better than intravenous systems because oral delivery does not confer risks of venous irritation. Submicron emulsions, also referred to as lipid emulsions or lipid microspheres, can reduce drug hydrolysis and improve drug bioavailability and efficacy.²⁸ Recently, increasing attention has been paid to addressing the difficulties associated with the undesirable oral bioavailability of drugs with poor water solubility through the use of submicron emulsions.^{29–32} Furthermore, submicron emulsions are suitable for industrial production due to their high drug loading capacity, ease of preparation and low cost.

In this study, we developed a drug-loaded submicron emulsion-based oral drug delivery system by high-pressure homogenization. A preparation process suitable for industrial-scale production was optimized. The formulation, liquiritigenin-loaded submicron emulsion (Lq-SE), was screened using a single-factor test in terms of particle size distribution, polydispersity index (PDI), zeta potential, pH value, contents, and entrapment efficiency (EE) and optimized by central composite design response surface methodology (CCD-RSM). Moreover, the gastrointestinal absorption characteristics and bioavailability of Lq-SE were investigated in rats. The protective effects of Lq-SE against DOX-induced cardiotoxicity were evaluated in nude mice, and the underlying mechanisms were also elucidated by investigating the involvement of modulation of the NADPH oxidase/ROS system, inhibition of MAPK kinase and NF- κ B activation, and reductions in DOX-mediated apoptosis. The findings will provide evidence for further clinical studies on DOX-induced cardiotoxicity and describe a novel drug delivery system for poorly water-soluble drugs.

Materials and Methods

Materials

The following materials were purchased or obtained from the sources in parentheses: Lq (Nanjing Shizhou Biotechnology Co., Ltd., Nanjing, China); egg lecithin (Lipoid E80) and medium-chain triglycerides (MCTs) (Lipoid KG, Ludwigshafen, Germany); soybean lecithin (EPIKURON 170, Degussa Food Ingredients, Germany); soybean oil (Zhejiang Tianyushan Medicinal Oil Co., Ltd., LongYou, China); poloxamer 188 (Pluronic F68[®]) (BASF AG, Ludwigshafen, Germany); glycerol (Shantou Jiahe Biotechnology Co., Ltd., Shantou, China); oleic acid (Xi'an Libang Pharmaceutical Co., Ltd., Xi'an, China); creatine

kinase (CK), creatine kinase isoenzymes (CK-MB), brain natriuretic peptide (BNP), atrial natriuretic peptide (ANP) and cardiac troponin-T (cTnT) kits (Nanjing Jiancheng Saihao Technology Co., Ltd.); interleukin-1 β (IL-1 β), interleukin 6 (IL-6), tumour necrosis factor- α (TNF- α), superoxide dismutase (SOD), and malondialdehyde (MDA) kits (Jiangsu Kaiji Biotechnology Co., Ltd., China); and ROS and glutathione (GSH) kits (Nanjing Jiancheng Bioengineering Institute). All chemicals and reagents used were of analytical or chromatographic grade. The animals used in this study were obtained from the Qinglong Mountain Animal Breeding Farm.

Preparation of Lq-SE

Lq-SE was prepared using high-pressure homogenization. Briefly, Lq, soybean lecithin and oleic acid were dispersed in a mixture of soybean oil and MCTs heated at 70°C to obtain a uniform aqueous phase. In addition, F68 and glycerol were dissolved in purified water maintained at 70°C to obtain the aqueous phase. Then, the oil phase was slowly injected into the aqueous phase under high-speed shear mixing at 15,000 rpm, and each sample was mixed for 3 min to obtain a coarse emulsion. The final emulsion was prepared by passing the coarse emulsion through a high-pressure homogenizer under a pressure of 1000 bar for 10 cycles. The pH value of the emulsion was adjusted to 5.0–6.0.

Optimization of the Homogenization Process

Homogenization factors such as the emulsifying temperature, homogenization pressure and cycle frequency were evaluated by a single-factor test using the mean particle size and size distribution as indicators. The emulsifying temperatures were set to 50, 60, and 70°C. The pressure was set from 500 to 100 bar, and the cycle frequency was 4–14. Finally, Lq-SE was prepared under optimal homogenization conditions to conduct the following property studies.

Optimization of the Preparative Formulation

First, in this study, the essential components in the formulation, including lecithin, the oil phase, and oleic acid, were investigated along with the pH value using a single-factor test under the same preparative conditions. Subsequently, CCD-RSM was used to optimize the formulation factors. The effects of oil phase content

(soybean oil and MCTs, X_1), emulsifier content (soy lecithin, X_2), and co-emulsifier content (F68, X_3) on the response variable (the average particle size, Y) were investigated. From preliminary studies, the following ranges of formulation factor values were considered: oil phase content (X_1), 10–30%; emulsifier content (X_2), 0.6–1.8%; and co-emulsifier content (X_3) of 0.1–0.6%. The experimental ranges and levels of factors are listed in Table 1. A total of 20 experiments were performed under the same conditions. The respective values and second-order polynomial equations were given by Design Expert 8.0.

Characterization of Submicron Emulsion Measurement of the Particle Size Distribution and Zeta Potential of Lq-SE

The particle size distribution, PDI and zeta potential of Lq-SE were measured using a Zetasizer Nano ZS90 (Malvern Instruments Corp., UK). Each sample was diluted with ultrapure water (1:5000 v/v) immediately at 25°C.

Content and EE of Lq-SE

The drug content of the submicron emulsion was determined by HPLC analysis. A total of 0.1 mL of emulsion (1 mg/mL) was collected and diluted to 50 mL with dehydrated alcohol to obtain the test sample. The samples were measured in a Tigerkin C8T column (4.6 mm \times 250 mm, 5 μ m) at 30°C with a 10 μ L injection volume. The mobile phase consisted of acetonitrile-water (40:60, v/v) pumped at a flow rate of 1.0 mL/min. The eluent was monitored at 274 nm.

The EE of Lq-SE, defined as the percentage of drug in the oil phase and interfacial film (which accounts for the total amount of drug in the emulsion) was calculated according to the following equation (Equation (1)):

$$EE(\%) = (C_{total}V_{total} - C_{water}V_{water})/C_{total}V_{total} \times 100\% \quad (1)$$

A 2 mL sample of Lq-SE was collected and ultracentrifuged at 40,000 rpm for 15 min to separate the oil phase and aqueous phase. The lower aqueous phase was extracted to measure the content of Lq by HPLC.³³

Pharmacokinetic Study

Animal Experiment

Female Sprague-Dawley rats weighing 200 \pm 20 g were obtained from the Qinglong Mountain Animal Breeding Farm. The animal experiments were performed according to the requirements in the Guide for the Humane Use and

Table 1 Central Composite Design for the Study of Three Independent Variables with the Experimental Results

Number	Coded Value of the Independent Variable			Actual Value of the Independent Variable			Response Value (Y)
	X ₁	X ₂	X ₃	Oil Phase Content (% w/v)	Emulsifier Content (% w/v)	Co-Emulsifier Content (% w/v)	Particle Size (nm)
1	-1	-1	-1	14.05	0.84	0.20	224.5
2	1	-1	-1	25.95	0.84	0.20	186.9
3	-1	1	-1	14.05	1.56	0.20	283.3
4	1	1	-1	25.95	1.56	0.20	256.0
5	-1	-1	1	14.05	0.84	0.50	181.9
6	1	-1	1	25.95	0.84	0.50	166.5
7	-1	1	1	14.05	1.56	0.50	243.0
8	1	1	1	25.95	1.56	0.50	220.5
9	-1.68	0.00	0.00	10.00	1.20	0.35	161.1
10	1.68	0.00	0.00	30.00	1.20	0.35	244.1
11	0.00	-1.68	0.00	20.00	0.60	0.35	214.1
12	0.00	1.68	0.00	20.00	1.80	0.35	188.9
13	0.00	0.00	-1.68	20.00	1.20	0.10	236.1
14	0.00	0.00	1.68	20.00	1.20	0.60	282.6
15	0.00	0.00	0.00	20.00	1.20	0.35	221.7
16	0.00	0.00	0.00	20.00	1.20	0.35	221.1
17	0.00	0.00	0.00	20.00	1.20	0.35	224.4
18	0.00	0.00	0.00	20.00	1.20	0.35	220.2
19	0.00	0.00	0.00	20.00	1.20	0.35	223.1
20	0.00	0.00	0.00	20.00	1.20	0.35	219.5

Care of Laboratory Animals were approved by the Animals Ethics Committee of the Nanjing University of Chinese Medicine. The approved protocol was “Scientific Protocol (2007) Number 16 of Nanjing University of Chinese Medicine”. The healthy rats were randomly divided into two groups of 6 rats each. Before starting the study, both groups were fasted overnight for 12 h with free access to water. One group was orally administered Lq-SE at a dose of 20 mg/kg, and the other group was administered Lq suspended in water. At each predetermined time point (3, 5, 10, 15, 30, 60, 120, 240, 360, 480, and 600 min), blood samples were collected and centrifuged at 1500 rpm for 5 min to separate serum.

LC-MS Quantification of Plasma Samples

Separate serum (100 μ L) and internal standard solution (10 μ L) aliquots were placed into 1.5 mL centrifuge tubes and vortexed for 30 s. Each sample was added to 500 μ L of acetonitrile, and the protein was precipitated by vortexing for 3 min and centrifugation at 12,000 rpm for 5 min. The supernatant was transferred to another centrifuge tube and

centrifuged again (12,000 rpm) for 5 min. The supernatant (2 μ L) was injected into the LC-MS system for analysis.

The mobile phase was composed of water and acetonitrile (A was water, and B was acetonitrile). The gradient elution was as follows: 0–1.0 min, 5–50% B; 1.0–3.0 min, 50–90% B; 3.0–4.0 min, 90% B; 4.0–5.0 min, 90–5% B; and 5.0–5.5 min, 5% B. The column flow rate was 0.3 mL/min with a 2 μ L injection volume. The column temperature was 35°C.

The parameters were as follows: ion source, electrospray ionization (ESI); curtain gas flow (CUR), 35; temperature (TEM), 500; ion spray voltage (IS), 5500; gas 1, 35; gas 2, 35; declustering potential (DP), -60.73; collision energy (CE), -33.03; entrance potential (EP), -12.87; and collision exit potential (CXP), -12.96. The ion pairs used for the analysis were m/z 255.0→119.0 (Lq) and m/z 269.0→117.0 (apigenin).

Animal Groups and Treatment

Male C57BL/6 mice (6–8 weeks old) were obtained from the Qinglong Mountain Animal Breeding Farm. The animal

experiments were performed according to the requirements in the Guide for the Humane Use and Care of Laboratory Animals and were approved by the Animals Ethics Committee of the University. The mice were randomly divided into the following five groups: the control group ($n = 8$), the model group ($n = 8$), and Lq-SE treatment groups administered low, medium, and high doses (10, 20, and 40 mg/kg, respectively) ($n = 24$). The treatment groups were pre-treated with Lq-SE (10, 20, or 40 mg/kg⁻¹) via intragastric administration once per day for 7 consecutive days. The control and model groups received saline instead of Lq-SE. The mice in the model and treatment groups were intraperitoneally administered 15 mg/kg DOX, and the mice in the control group were injected with the same volumes of physiological saline. Then, the mice in the treatment groups were given Lq-SE for 5 consecutive days after the model was established. At the end of the experiment, the mice were sacrificed by exsanguination 1 h after the beginning of Lq-SE or saline administration. Serum samples and heart tissues were collected for biochemical analysis, pathological staining, and Western blot assays.

Biochemical Analysis

At the end of the experiments, blood samples were collected, and serum was obtained by centrifugation. CK, CK-MB, ANP, BNP and cTnT are important serum-specific markers used to assess cardiac dysfunction. The activity of these molecules and of SOD, GSH and MDA was measured using applicable ELISA kits according to the manufacturer's instructions. TNF- α , IL-6 and IL 1 β in serum were also examined with corresponding detection kits according to the manufacturer's instructions.

ROS Measurements

ROS measurement was carried out using freshly dissected heart tissues. Samples (50 mg of protein) were incubated with 10 mL of DCF-DA (10 mM) for 2 h at 37°C. The levels of production of intracellular ROS, including superoxide anions (O²⁻), hydroxyl radicals (\cdot OH), hydrogen peroxide (H₂O₂), and peroxides, were determined using a total ROS detection kit according to the manufacturer's instructions. The fluorescence of the produced intracellular ROS was ultimately measured using a microplate reader (MD SpectraMax M3, USA) with an emission wavelength of 525 nm and an excitation wavelength of 500 nm. The change in fluorescence was detected as an arbitrary unit.

Histopathologic Assay

Heart tissues were fixed in 10% formalin and embedded in paraffin for 24 h, and then the sections (4 μ m thick) were stained with haematoxylin-eosin (H&E) solution at room temperature (0.5% haematoxylin for 5 min and 0.1% eosin for 1 min). Finally, images of the stained sections were obtained using a light microscope (Olympus BX41, Japan).

Western Blot Analysis

Heart samples were homogenized in lysis buffer to yield a homogenate. Then, final supernatants from the hearts were obtained by centrifugation at 12,000 rpm for 10 min at 4°C. The protein concentrations were determined using a BCA protein assay kit (Jiangsu Kaiji Biotechnology Co., Ltd.) with bovine serum albumin as a standard. Equal amounts of total protein were subjected to 10–12% sodium dodecyl sulfate–polyacrylamide electrophoresis (SDS-PAGE) (Jiangsu Kaiji Biotechnology Co., Ltd., China) and transferred to polyvinylidene fluoride (PVDF) membranes. The membranes were blocked with 5% skim milk in TBS-T for 1 h at room temperature and then probed with primary antibodies at 4°C with gentle shaking overnight. The protein bands were observed using enhanced chemiluminescence (ECL) and imaged using a G:BOX ChemiXR5 imaging system. The expression level of each protein was defined as the grey value using Gel-Pro32 software. NOX2 (1:5000), NF- κ B p65 (1:1000), NF- κ B p65 (phospho-S536, 1:2000), I κ B α (1:5000), and I κ B α (phospho-S36, 1:10,000) antibodies were purchased from Abcam (USA). GAPDH (1:10,000) and Enos (1:500) antibodies were purchased from Jiangsu Kaiji Biotechnology Co., Ltd. (China). JNK (1:1000), p-JNK (1:1000), ERK1/2 (1:1000), and p-ERK1/2 (1:1000) antibodies were purchased Cell Signaling Technology (USA). NOX4 (1:200), p38 (1:200), and p-p38 (1:200) antibodies were purchased from Beijing Bioss Biotechnology Co., Ltd. (China). Bax and Bcl (1:200) antibodies were purchased from Santa Cruz Biotechnology (USA). Caspase-3 (1:500) antibodies were purchased from Proteintech Group (USA).

Statistical Analysis

All data are expressed as the mean \pm standard deviation (SD). Statistical analysis was performed using ANOVA with a statistical significance threshold of $P < 0.05$.

Calculations were made using GraphPad Prism 8.0 (GraphPad, San Diego, CA, USA).

Results

Optimization of the Homogenization Process

The homogenization process can affect the quality of Lq-SE during manufacturing. Homogenization pressure, temperature, and frequency are important parameters that control the size distribution and stability of the emulsion. As shown in Figure 2A, increasing the preparation temperature of the coarse emulsion decreased the particle size of Lq-SE,

which exhibited particle diameters of 200 to 220 nm at 70°C. Additionally, the formed droplets were smaller in diameter at a pressure of 1000 bar and a homogenization frequency of 10 than at other pressures or frequencies (Figure 2B and C). Finally, we chose the homogenization preparation conditions of 70°C, 1000 bar, and a 10× homogenization frequency for use in further studies.

Optimization of the Lq-SE Formulation

The formulation of Lq-SE was screened using a single-factor test. Studies investigating both the thermal sterilization stability and storage stability at 40°C were carried out,

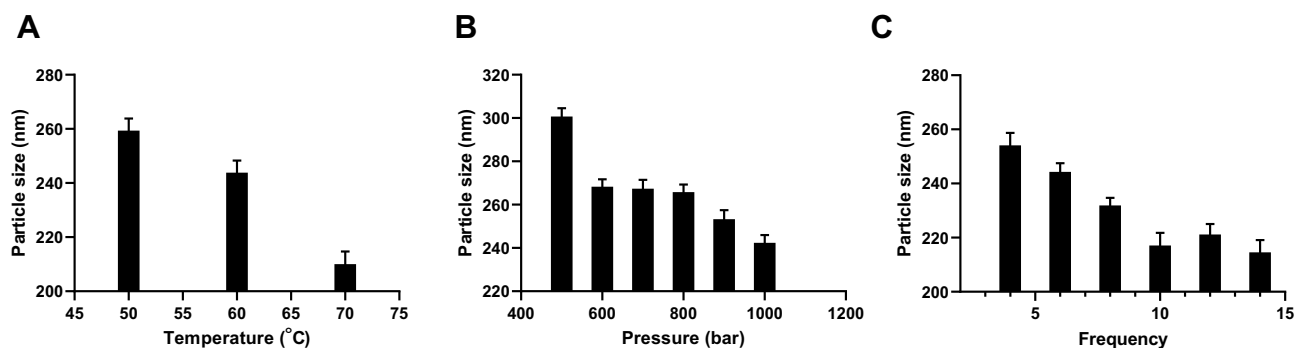


Figure 2 Investigation of the homogenization process with different (A) temperatures, (B) pressures, and (C) frequencies.

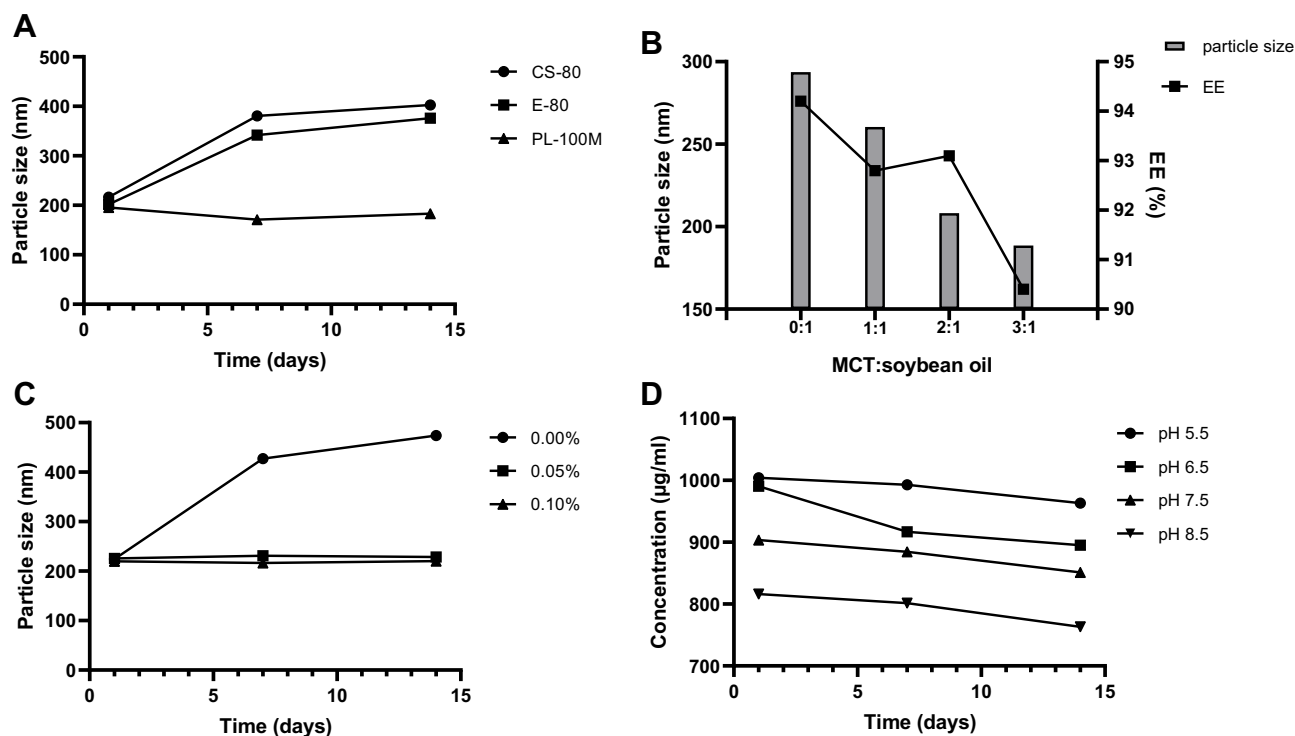


Figure 3 Optimization of the following components of the formulation by single-factor tests: (A) The lecithin used, (B) The soybean oil:MCT ratio, (C) The oleic acid concentration, and (D) The pH value.

and the particle size distribution, pH value, contents, and EE were evaluated. The lecithin and oil phases are essential components in the formulation and significantly influence the properties and stability of emulsions.³⁴ The use of different types of lecithin in the formulation was investigated. The results are shown in [Figure 3A](#). Compared with those of CS-80- and E-80-containing formulations, the particle sizes of PL-100M-containing formulations remained unchanged, maintaining stable quality at 40°C for 2 weeks. Therefore, PL-100M was selected as the optimal emulsifier for the formulations. As shown in [Figure 3B](#), because of the low viscosity of MCT, the oil phase reduces the size of the emulsion by increasing the proportion of MCT. Besides, the increase of MCT leads to the difficulty of emulsification and the decrease of EE. The mixture of soybean oil-MCT (1:2, w/w) was selected as the optimized oil phase with favorable EE and lower particle size. [Figure 3C](#) and [D](#) shows that 0.05% oleic acid (w/v) and a pH value of 5.5 conferred good stability to Lq-SE at 40°C for 2 weeks. Therefore, PL-100M, a soybean oil/MCT mixture (1:2, w/w), 0.05% oleic acid (w/v) and a pH value of 5.5 were employed in this study.

CCD-RSM is a useful statistical tool to optimize important factors among several variables in a medium. The Lq-SE formulation consists of an oil phase, an emulsifier, and a co-emulsifier. In the present study, 20 experimental replicates were conducted between the response variable (Y) and the three independent variables (X_1 , X_2 , X_3), as shown in [Table 1](#). The particle size (Y) acted as a dependent variable in the responses of experimental factors involving the contents of the oil phase (X_1), soy lecithin (X_2), and F68 (X_3) (independent variables). Multiple non-linear regression analysis and estimation of coefficients were performed with software. The following polynomial equation (Equation (2)) with a correlation coefficient of 0.9972 was generated:

$$Y = 99.982 + 13.274X_1 + 93.126X_2 - 512.052X_3 - 0.754X_1 \cdot X_2 + 0.451X_1 \cdot X_3 + 63.448X_2 \cdot X_3 - 0.195X_1^2 - 57.258X_2^2 + 592.567X_3^2 \quad (2)$$

To obtain a better understanding of the effects of the three formulation factors and their interactions on the particle size, 3-dimensional (3D) response surface plots were made between the dependent and independent variables with Expert 8.0.6 software, as shown in [Figure 4](#). These graphs show the effects of the soybean oil/MCT mixture (1:2, w/w) (X_1), soybean lecithin content (X_2) and F68 content (X_3) on particle size (Y) when the third independent variable was centrally located.

When the soybean oil/MCT mixture (1:2, w/w) was at the centre level, the minimum particle size was achieved with a maximum level of soybean lecithin and a minimum level of F68. The optimal levels of the experimental factors in Lq-SE that yielded a desirable particle size were 20.0% (w/v) soybean oil/MCT (1:2, w/w) mixture, 1.2% (w/v) soybean lecithin and 0.3% (w/v) F68. Under these optimal factors, the particle size in our formulation was 221.7 nm.

Characterization of Lq-SE

[Figure 5A](#) is a schematic illustration of Lq-SE droplets. The particle size distribution, PDI and zeta potential of Lq-SE were analysed by a laser light scanning instrument. The mean particle size of Lq-SE droplets was 221.7 ± 5.80 nm with a narrow distribution, and Lq-SE had a small PDI of 0.106 ± 0.068 ([Figure 5B](#)). The zeta potential of Lq-SE was determined to be -28.23 ± 0.42 mV, which was closely correlated with the stability of Lq-SE.

Pharmacokinetic Study

The pharmacokinetic experiment compared the relative bioavailability of Lq and Lq-SE in rats after oral administration. The mean plasma concentration-time profiles of Lq and Lq-SE are presented in [Figure 6](#). The pharmacokinetic results in rats showed that Lq and Lq-SE were absorbed rapidly in vivo after oral administration. The Lq-SE concentration was significantly higher than the Lq concentration. The plasma peak concentration of Lq-SE was 2831.17 ng/mL, over 13.43-fold that of Lq (210.84 ng/mL). Moreover, the area under the curve (AUC) of Lq-SE was 595% higher than that of Lq. The results showed that the use of the Lq-SE delivery system was an effective approach to promote the absorption and bioavailability of Lq in rats. The main pharmacokinetic parameters were also summarized with DAS 2.0 software. The results are shown in [Table 2](#).

Lq-SE Alleviates Myocardial Injury in vivo

Serum biochemical markers of cardiac injuries were assayed, including CK, CK-MB, ANP, BNP, and cTnT. As shown in [Figure 7A](#), compared with the control groups, the model group had obviously increased serum CK and CK-MB levels ($P < 0.01$, $P < 0.01$). However, treatment with Lq-SE (20 or 40 mg/kg) markedly decreased the serum levels of CK and CK-MB ($P < 0.05$, $P < 0.01$). Moreover, the serum levels of ANP, BNP, and cTnT in the group treated with Lq-SE (40 mg/kg) were significantly lower than those in the model group ([Figure 7B](#)). In addition, histopathological examination of heart tissue showed histological changes in the model

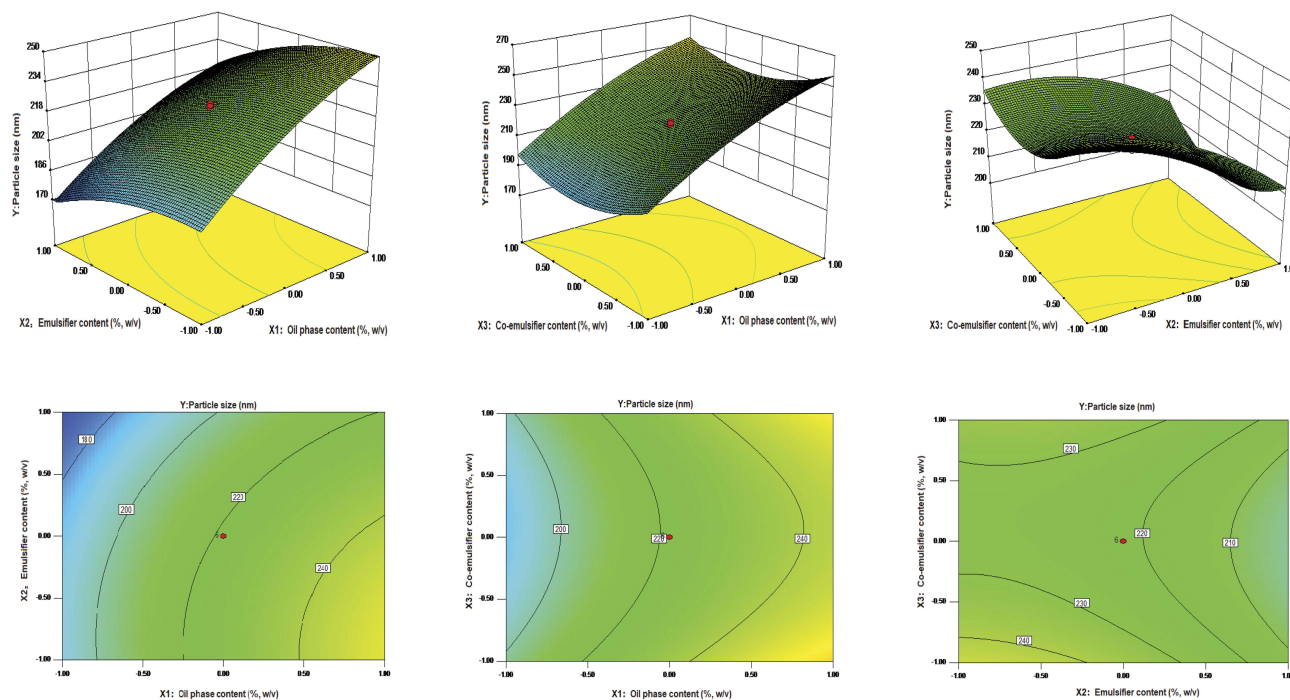


Figure 4 Response surface plot showing the influence of the oil phase (X_1), emulsifier (X_2), and poloxamer 188 (X_3) on particle size (Y).

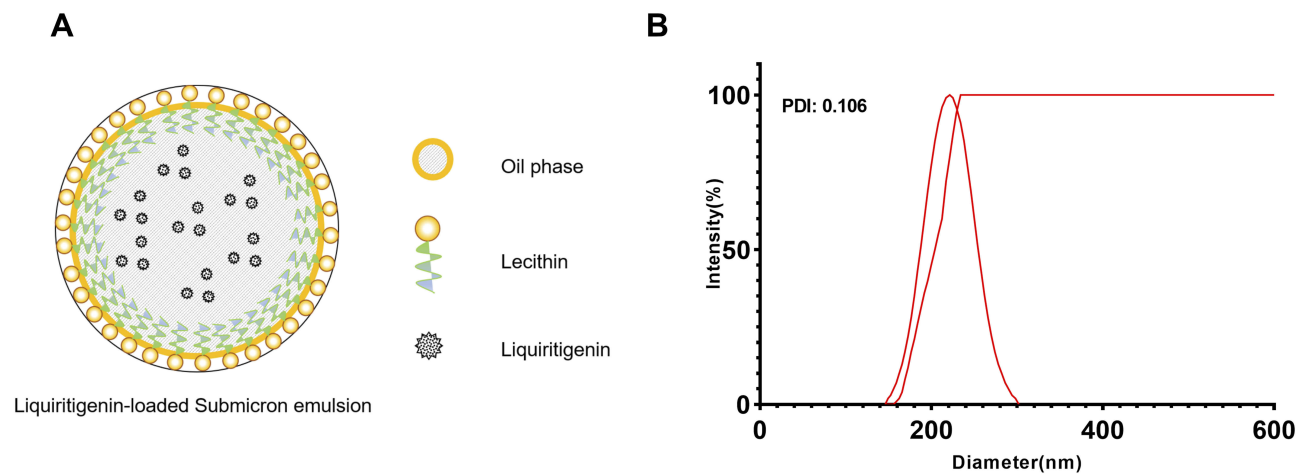


Figure 5 (A) Schematic illustration of Lq-SE droplets. (B) Particle size distribution spectrum for Lq-SE.

group, including obviously disordered myocardial tissue texture, pyknosis and disrupted plasma; these changes were attenuated in the groups treated with the medium and high doses of Lq-SE (Figure 7C). These results indicate that Lq-SE significantly attenuates the cardiac injury caused by DOX.

Lq-SE Alleviates Oxidative Damage in vivo

Normally, under the action of various oxidative and antioxidant enzymes, ROS are in a dynamic equilibrium state in vivo. After stimulation, excessive ROS levels result in

oxidative stress reactions and tissue damage. As shown in Figure 8, we found that SOD and GSH levels were significantly decreased ($P < 0.01$) and that ROS and MDA levels were increased ($p < 0.01$) in the model group compared with the control group. Moreover, the activity of SOD and GSH was significantly increased ($P < 0.01$) in the medium- and high-dose Lq-SE groups compared with the model group, while the content of ROS and the levels of MDA were significantly decreased ($P < 0.01$). Furthermore, the protein expression of NOX2 and NOX4 was significantly inhibited

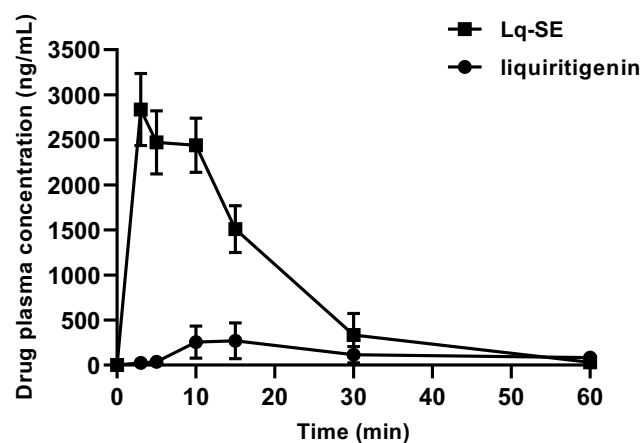


Figure 6 Plasma concentration-time curve in rats after oral administration of Lq and Lq-SE.

Table 2 Pharmacokinetic Parameters of Lq and Lq-SE (20 mg/kg, Oral) in Rats (n = 6)

Parameters	Liquiritigenin	Lq-SE
$t_{1/2}$ (min)	12.63 ± 3.85	8.64 ± 2.52
T_{max} (min)	17.48 ± 5.24	4.74 ± 1.33
C_{max} (ng/mL)	210.84 ± 58.57	2831.17 ± 427.38**
AUC_{0-t} (ng/mL×min)	8586.91 ± 1758.85	51082.00 ± 14281.73**

Notes: The data are expressed as the mean ± SD. **P < 0.01 versus Lq.

Abbreviations: DOX, doxorubicin; EE, entrapment efficiency; F68, poloxamer 188; MCT, medium chain triglyceride; CK, creatine kinase; CK-MB, creatine kinase isoenzyme; BNP, brain natriuretic peptide; ANP, atrial natriuretic peptide; cTnT, cardiac isoform of Troponin T; ROS, reactive oxygen species; SOD, superoxide dismutase; GSH, glutathione; MDA, malondialdehyde; IL-6, interleukin 6; IL-1 β , interleukin 1 β ; TNF- α , tumor necrosis factor- α ; MAPK, mitogen-activated protein kinase; NF- κ B, nuclear factor- κ B; I κ B α , kappa B-alpha; JNK, c-Jun N-terminal kinase; pJNK, phosphorylated c-Jun N-terminal kinase; ERK, signal-regulated kinase; Bax, Bcl-2-associated X protein; Bcl-2, B-cell lymphoma 2; C-caspase 3, cleaved-caspase 3; GAPDH, glyceraldehyde 3-phosphate dehydrogenase.

in the high-dose group ($P < 0.01$). These results suggest that Lq-SE has a significant antioxidant effect that is related to activation of SOD and GSH and inhibition of NOX2 and NOX4 expression.

Lq-SE Reduces DOX-Induced Inflammation in Cardiac Tissue

DOX can cause oxidative damage and myocardial toxicity, which often induce inflammation in the body and the release of large numbers of inflammatory factors to aggravate tissue damage, resulting in a vicious cycle.

As shown in Figure 9A, the levels of IL-1 β , IL-6 and TNF- α in the plasma were significantly higher in the model group ($P < 0.01$, $P < 0.05$, and $P < 0.05$, respectively) than in the control group. Compared with those in the model group, the levels of IL-6 and TNF- α were significantly decreased in the low- and

medium-dose groups ($P < 0.01$, $P < 0.05$), and the levels of IL-6, IL-1 β and TNF- α were significantly decreased in the medium- and high-dose groups ($P < 0.01$).

In addition, the protein expression levels of p65 and I κ B α , components of the NF- κ B pathway, were upregulated in the model group. The protein expression of p65 and I κ B α was significantly inhibited in the high- and medium-dose Lq-SE groups ($P < 0.01$ and $P < 0.05$, respectively). The results demonstrate that Lq-SE reduces the inflammatory response via NF- κ B signalling (Figure 9B and C).

Lq-SE Protected Against DOX-Induced Apoptosis

To further study the myocardial protective mechanism of Lq-SE, we investigated apoptosis of myocardial cells. As shown in Figure 10, compared with the control condition, DOX treatment significantly decreased the expression of Bcl-2 protein ($P < 0.01$) and increased the expression of Bax and c-caspase-3 protein ($P < 0.05$). Compared with the model group, the high-dose Lq-SE group showed increased Bcl-2 protein expression ($P < 0.05$) and decreased Bax and c-caspase-3 protein expression ($P < 0.05$).

In addition, we found that the expression of JNK, ERK, and phosphorylated p38, components of the MAPK pathway, was significantly increased ($P < 0.01$) in the model group, whereas the expression of JNK, ERK and p38 protein was inhibited in the low-, middle- and high-dose Lq-SE groups ($P < 0.05$, $P < 0.01$, and $P < 0.01$, respectively) in a dose-dependent manner.

Discussion

More than 40% of compounds have low oral bioavailability due to poor dissolution or poor permeability.³⁵ Upon oral administration, dissolution of a drug molecule is the first step in the absorption process. Submicron emulsions are receiving increasing attention as delivery systems for compounds with low aqueous solubility and lipid solubility. Our results indicate that the Lq-loaded submicron emulsion system significantly increased the bioavailability of Lq, resulting in higher drug plasma concentrations after oral administration than treatment with Lq suspension.

DOX is one of the most effective chemotherapeutic drugs used to treat cancer.³⁶ However, DOX-induced cardiotoxicity remains a major challenge in clinical patients. Thus, it is necessary to find a preventive treatment for DOX-induced cardiotoxicity.³⁷ Previous studies have demonstrated that

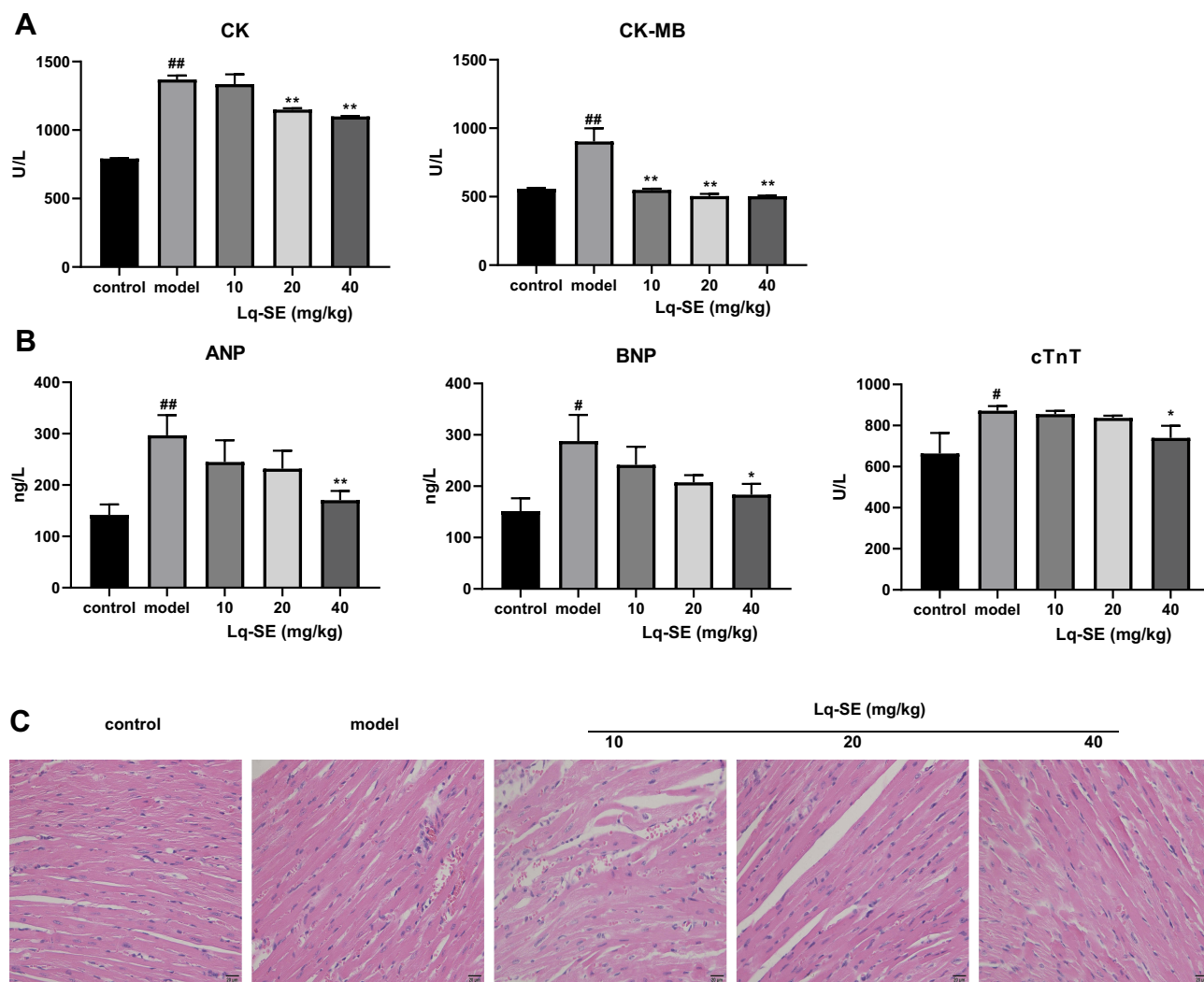


Figure 7 Effects of Lq-SE on DOX-induced changes in serum heart injury biomarkers. **(A)** CK and CK-MB levels in mouse serum. **(B)** ANP, BNP, and cTnT levels. **(C)** H&E staining images showing the effects of Lq-SE on heart tissues in mice (200× magnification). The results are presented as the mean ± SEM for 8 animals in each group. [#]P < 0.05 and ^{###}P < 0.01 versus the control group; ^{*}P < 0.05 and ^{**}P < 0.01 versus the DOX group.

oxidative stress plays a critical role in the pathogenesis of DOX-induced cardiotoxicity.^{38,39} The reaction that combines hydrogen and O^{2-} to form H_2O_2 can be slowed by some antioxidant enzymes, such as GSH, GSH-Px and SOD.⁴⁰ Suppression of ROS production can alleviate apoptosis, necrosis, and autophagy associated with DOX-induced cardiotoxicity.^{41,42} ROS derived from NADPH oxidase are major contributors to the cardiac injury caused by DOX.⁴³ In the present study, pretreatment with Lq-SE significantly decreased ROS and MDA levels, increased SOD and GSH levels and suppressed NOX4 and NOX2 protein expression. Therefore, the present study demonstrates that Lq-SE possesses antioxidative properties and protects against DOX-induced cardiotoxicity by scavenging ROS through inhibition of NOX2 and NOX4 enzyme activity.

The MAPK signalling pathway can be mediated by multiple stress factors involved in cell proliferation, differentiation, and death and is related to protective effects against cardiomyocyte death.⁴⁴ DOX can induce oxidative stress to activate the MAPK signalling pathway and further activate the phosphorylation of apoptotic proteins, leading to myocardial toxicity in rats.⁴⁵ In addition, DOX activates the NF- κ B signalling pathway by phosphorylating and degrading I κ B α protein; NF- κ B then enters the nucleus to release inflammatory factors and induce cardiomyocyte apoptosis.⁴⁶ Previous research has demonstrated that DOX induces inflammatory reactions and stimulates the release of proinflammatory mediators such as TNF- α , IL-1 β , and IL-6, which causes pathological alterations during the development of cardiomyopathy.^{47,48} One study has demonstrated that cardioprotective activity is improved by

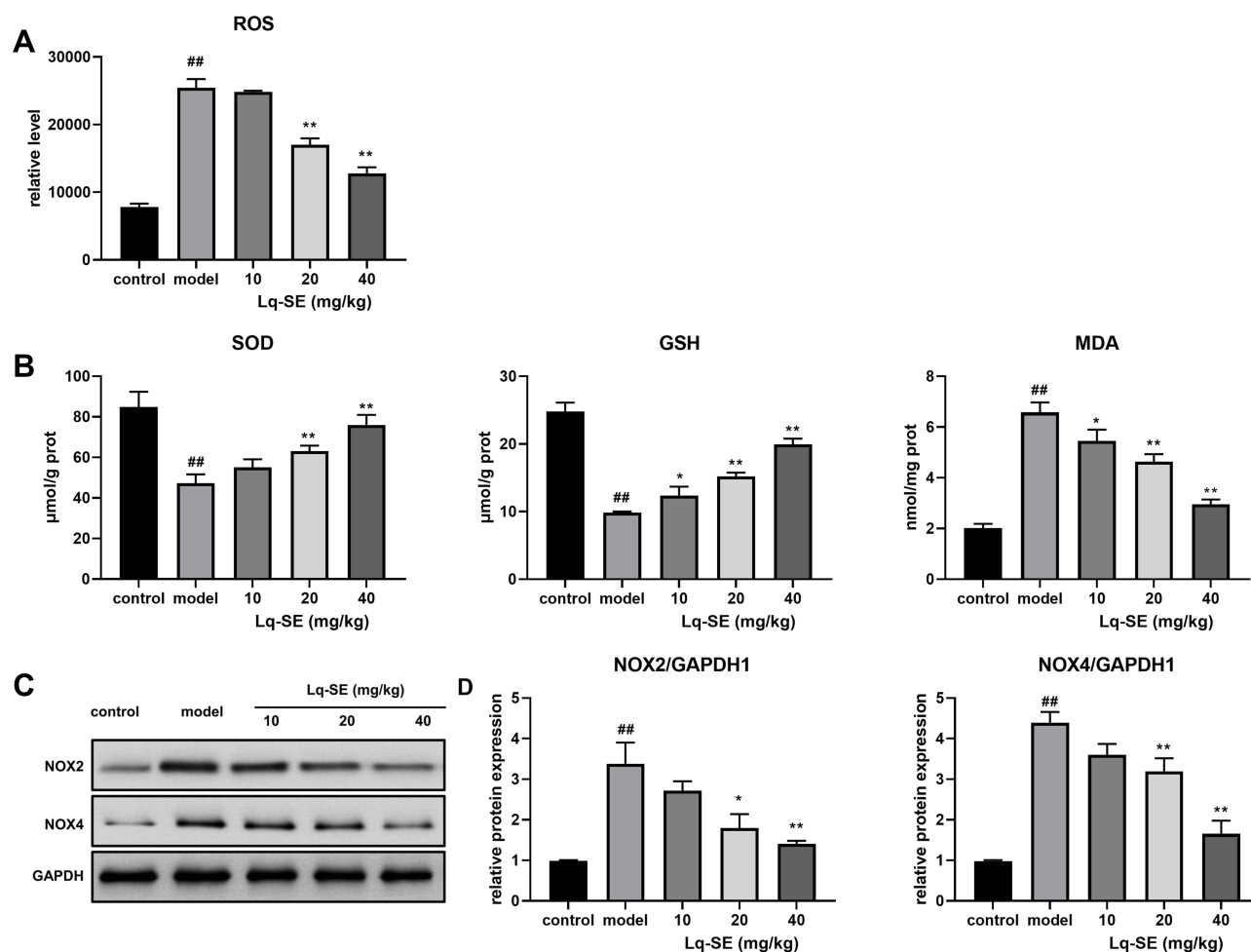


Figure 8 Lq-SE treatment reduces the oxidative stress induced by DOX in mice. **(A)** Effects of Lq-SE on ROS production in heart tissues. **(B)** SOD levels, GSH levels, and MDA levels in serum were determined by ELISA. **(C)** Representative Western blot images of NOX4 and NOX2 protein expression. **(D)** Effects of Lq-SE on NOX2 and NOX4 protein expression in mice. ^{###}*P* < 0.01 versus the control group; ^{*}*P* < 0.05 and ^{**}*P* < 0.01 versus the DOX group.

inhibition of MAPK/NF- κ B signalling and subsequent inhibition of inflammatory mediators.⁴⁹ In the present study, we observed that pretreatment with Lq-SE significantly inhibited the production of the proinflammatory cytokines IL-1, IL-6 and TNF- α and suppressed the phosphorylation of the p65 and I κ B α proteins. In addition, the phosphorylation levels of the MAPK isoforms (p38, JNK, and ERK) were dramatically decreased after Lq-SE pretreatment. Therefore, the protective effects of Lq-SE against DOX-induced cardiotoxicity are mediated via inhibition of the MAPK/NF- κ B signalling pathway.

Increasing evidence has revealed that the apoptosis and autophagy of cardiomyocytes play significant roles in DOX-induced cardiotoxicity.^{50,51} Apoptosis is modulated by proapoptotic and anti-apoptotic components; among these, Bax is an important proapoptotic protein, while Bcl-2 is anti-apoptotic.⁵² Research has shown that DOX induces apoptosis

by promoting Cytc release from mitochondria and by regulating Bcl-2 and Bax.⁵³ Our data indicate that the protective effects of Lq-SE involve significant reductions in caspase-3 activation and Bax expression and promotion of Bcl-2 expression, which attenuate the apoptosis caused by DOX. These results show the cardioprotective mechanisms of Lq-SE against DOX-induced cardiotoxicity, which include antioxidant, anti-inflammatory, and anti-apoptotic activity. The formulation of submicron emulsion is considered low cytotoxicity as reported in the literature.^{54,55} Further stability tests and toxicological studies are required for the potential clinical application.

Conclusion

In conclusion, we have developed a novel drug delivery system, Lq-SE, to enhance the bioavailability of Lq. Our results demonstrate that Lq-SE significantly decreases DOX-induced

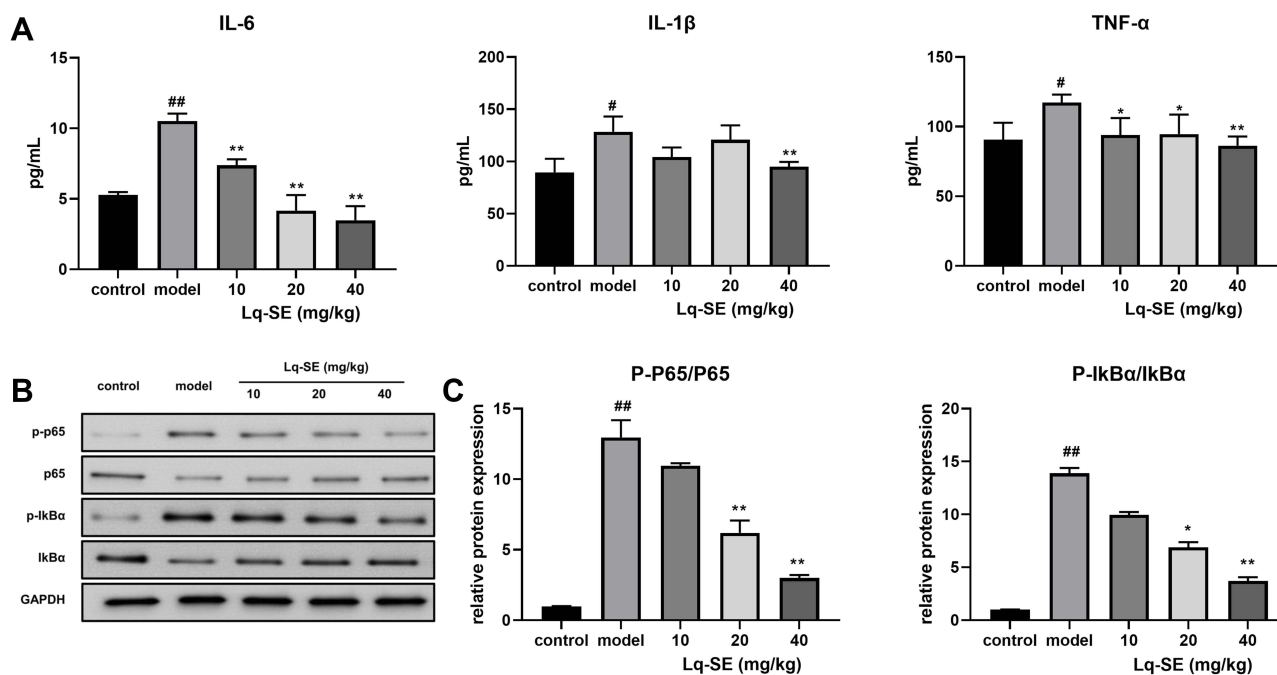


Figure 9 Lq-SE treatment suppresses cardiac inflammation induced by DOX in mice. **(A)** IL-6 levels, IL-1β levels, and TNF-α levels in hearts were determined by ELISA (n=8). **(B)** Representative Western blot images of p65, p-p65, p-IκBα, and IκBα protein expression. **(C)** The band densities were quantified and normalized to the band density of GAPDH, and the values given are the means ± SDs (n = 3). # P < 0.05 and ## P < 0.01 versus the control group; *P < 0.05 and **P < 0.01 versus the DOX group.

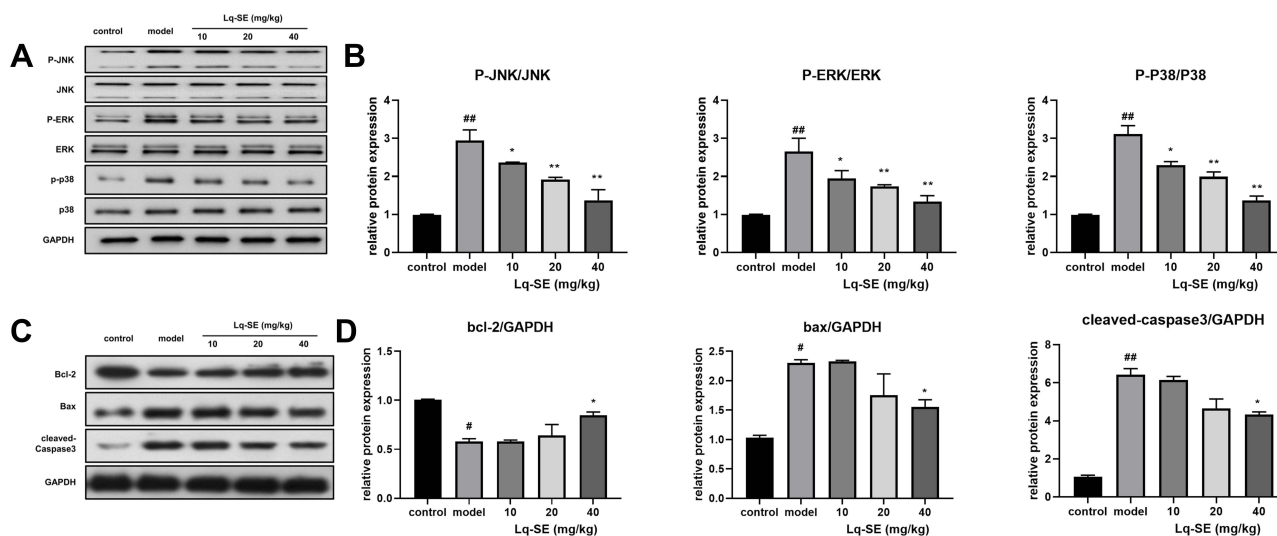


Figure 10 **(A)** Representative Western blot images of p-JNK, JNK, p-ERK, ERK, p-p38, and p38 protein expression. **(B)** The band densities were quantified and normalized to the band density of GAPDH. **(C)** Representative Western blot images of Bcl-2, Bax, and c-caspase-3 protein expression. **(D)** The band densities were quantified and normalized to the band density of GAPDH. All values given are the means ± SDs (n = 3). #P < 0.05 and ##P < 0.01 versus the control group; *P < 0.05 and **P < 0.01 versus the DOX group.

cardiotoxicity in mice. This mechanism by which Lq-SE reduces DOX-induced cardiotoxicity possibly involves modulation of the NADPH oxidase/ROS system, inhibition of the MAPK/NF-κB signalling pathway and reductions in

DOX-mediated apoptosis (Figure 11). Therefore, Lq-SE could potentially exhibit a cardioprotective effect during chemotherapy involving DOX to enable better patient compliance. Further study is needed to elucidate the underlying

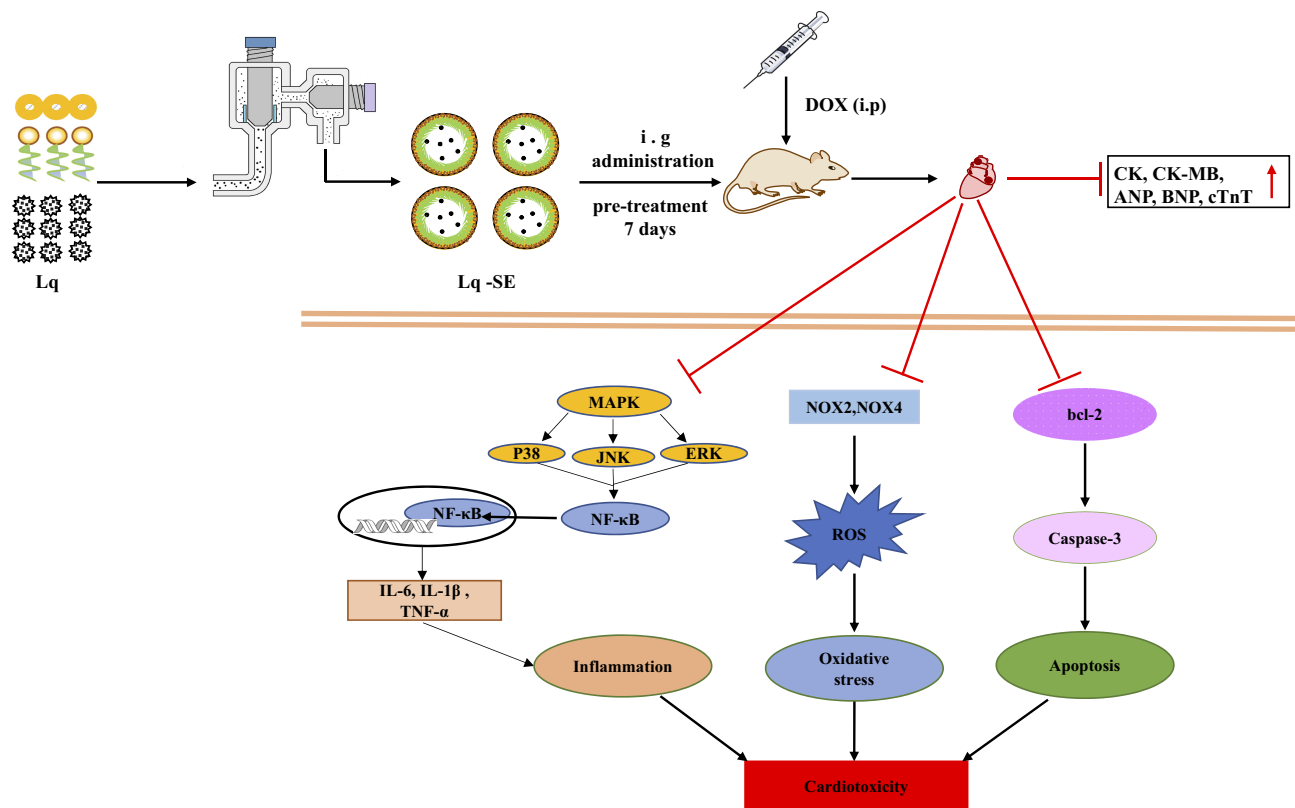


Figure 11 A working model of the effects of Lq-SE on DOX-induced cardiotoxicity. Lq-SE protects against DOX-induced cardiotoxicity via antioxidant, anti-inflammatory, and anti-apoptotic activity.

mechanism of the cardioprotective effect of Lq-SE against DOX-induced cardiotoxicity.

Acknowledgments

The authors are grateful for financial support for this work from the National Science Foundation of China (81873004 and 81873287), the State Project for Essential Drug Research and Development (2017ZX09301075), the Key Project of Natural Science Research in Colleges and Universities in Jiangsu Province (18KJA360009), and the Technology Project of the Chinese Medicine Agency of Jiangsu Province (PY201518).

Disclosure

The authors report no conflicts of interest in this work.

References

- Renu K, Abilash VG, Tirupathi Pichiah PB, Arunachalam S. Molecular mechanism of doxorubicin-induced cardiomyopathy – an update. *Eur J Pharmacol*. 2018;818:241–253. doi:10.1016/j.ejphar.2017.10.043
- Damiani RM, Moura DJ, Viau CM, Caceras RA, Henriques JAP, Saffi J. Pathways of cardiac toxicity: comparison between chemotherapeutic drugs doxorubicin and mitoxantrone. *Arch Toxicol*. 2016;90(9):2063–2076. doi:10.1007/s00204-016-1759-y
- Barry E, Alvarez JA, Scully RE, Miller TL, Lipshultz SE. Anthracycline-induced cardiotoxicity: course, pathophysiology, prevention and management. *Expert Opin Pharmacother*. 2007;8(8):1039–1058. doi:10.1517/14656566.8.8.1039
- Lipshultz SE, Alvarez JA, Scully RE. Anthracycline associated cardiotoxicity in survivors of childhood cancer. *Heart*. 2008;94(4):525–533. doi:10.1136/hrt.2007.136093
- Lipshultz SE, Miller TL, Scully RE, et al. Changes in cardiac biomarkers during doxorubicin treatment of pediatric patients with high-risk acute lymphoblastic leukemia: associations with long-term echocardiographic outcomes. *J Clin Oncol*. 2012;30(10):1042–1049. doi:10.1200/JCO.2010.30.3404
- Pugazhendhi A, Edison TNJI, Velmurugan BK, Jacob JA, Karuppusamy I. Toxicity of Doxorubicin (Dox) to different experimental organ systems. *Life Sci*. 2018;200:26–30. doi:10.1016/j.lfs.2018.03.023
- Mitry MA, Edwards JG. Doxorubicin induced heart failure: phenotype and molecular mechanisms. *Int J Cardiol Heart Vasc*. 2016;10:17–24. doi:10.1016/j.ijcha.2015.11.004
- Gorini S, De Angelis A, Berrino L, Malara N, Rosano G, Ferraro E. Chemotherapeutic drugs and mitochondrial dysfunction: focus on doxorubicin, trastuzumab, and sunitinib. *Oxid Med Cell Longev*. 2018;2018:1–15. doi:10.1155/2018/7582730
- Broeyer FJF, Osanto S, Suzuki J, et al. Evaluation of lecithinized human recombinant super oxide dismutase as cardioprotectant in anthracycline-treated breast cancer patients. *Br J Clin Pharmacol*. 2014;78(5):950–960. doi:10.1111/bcp.12429
- Vincent DT, Ibrahim YF, Espey MG, Suzuki YJ. The role of antioxidants in the era of cardio-oncology. *Cancer Chemother Pharmacol*. 2013;72(6):1157–1168. doi:10.1007/s00280-013-2260-4

11. Zheng K, Li R, Zhou X, et al. Dual actions of albumin packaging and tumor targeting enhance the antitumor efficacy and reduce the cardiotoxicity of doxorubicin in vivo. *Int J Nanomedicine*. 2015;10:5327–5342. doi:10.2147/IJN.S84478
12. Zhang D, Xu Q, Wang N, et al. A complex micellar system co-delivering curcumin with doxorubicin against cardiotoxicity and tumor growth. *Int J Nanomedicine*. 2018;13:4549–4561. doi:10.2147/IJN.S170067
13. Rahman AM, Yusuf SW, Ewer MS. Anthracycline-induced cardiotoxicity and the cardiac-sparing effect of liposomal formulation. *Int J Nanomedicine*. 2007;2:567–583.
14. Fang Y, Wang H, Dou H-J, et al. Doxorubicin-loaded dextran-based nano-carriers for highly efficient inhibition of lymphoma cell growth and synchronous reduction of cardiac toxicity. *Int J Nanomedicine*. 2018;13:5673–5683. doi:10.2147/IJN.S161203
15. Yu J, Wang C, Kong Q, Wu X, Lu -J-J, Chen X. Recent progress in doxorubicin-induced cardiotoxicity and protective potential of natural products. *Phytomedicine*. 2018;40:125–139. doi:10.1016/j.phymed.2018.01.009
16. Huang L, Zheng M, Zhou Y, et al. Tanshinone IIA attenuates cardiac dysfunction in endotoxin-induced septic mice via inhibition of NADPH oxidase 2-related signaling pathway. *Int Immunopharmacol*. 2015;28(1):444–449. doi:10.1016/j.intimp.2015.07.004
17. Yu J, Gao H, Wu C, Xu Q-M, Lu -J-J, Chen X. Diethyl blechnic, a novel natural product isolated from *Salvia miltiorrhiza bunge*, inhibits doxorubicin-induced apoptosis by inhibiting ROS and activating JNK1/2. *IJMS*. 2018;19(6):1809. doi:10.3390/ijms19061809
18. Ogawa Y, Oku H, Iwaoka E, Iinuma M, Ishiguro K. Allergy-preventive flavonoids from *Xanthorrhoea hastilis*. *Chem Pharm Bull*. 2007;55(4):675–678. doi:10.1248/cpb.55.675
19. Kim YW, Zhao RJ, Park SJ, et al. Anti-inflammatory effects of liquiritigenin as a consequence of the inhibition of NF- κ B-dependent iNOS and proinflammatory cytokines production. *Br J Pharmacol*. 2008;154(1):165–173. doi:10.1038/bjp.2008.79
20. Jung EH, Lee J-H, Kim SC, Kim YW. AMPK activation by liquiritigenin inhibited oxidative hepatic injury and mitochondrial dysfunction induced by nutrition deprivation as mediated with induction of farnesoid X receptor. *Eur J Nutr*. 2017;56(2):635–647. doi:10.1007/s00394-015-1107-7
21. Kim YW, Ki SH, Lee JR, et al. Liquiritigenin, an aglycone of liquiritin in *Glycyrrhizae radix*, prevents acute liver injuries in rats induced by acetaminophen with or without buthionine sulfoximine. *Chem Biol Interact*. 2006;161(2):125–138. doi:10.1016/j.cbi.2006.03.008
22. Wätjen W, Weber N, Lou Y-J, et al. Prenylation enhances cytotoxicity of apigenin and liquiritigenin in rat H4IIE hepatoma and C6 glioma cells. *Food Chem Toxicol*. 2007;45(1):119–124. doi:10.1016/j.fct.2006.08.008
23. Zhang S, Zhou Y, Liu Y, Cai Y. Effect of liquiritigenin, a flavanone existed from *radix glycyrrhizae* on pro-apoptotic in SMMC-7721 cells. *Food Chem Toxicol*. 2009;47(4):693–701. doi:10.1016/j.fct.2008.12.015
24. Liu C, Wang Y, Xie S, et al. Liquiritigenin induces mitochondria-mediated apoptosis via cytochrome c release and caspases activation in HeLa Cells. *Phytother Res*. 2011;25(2):277–283. doi:10.1002/ptr.3259
25. Kim SC, Byun SH, Yang CH, Kim CY, Kim JW, Kim SG. Cytoprotective effects of *glycyrrhizae radix* extract and its active component liquiritigenin against cadmium-induced toxicity (effects on bad translocation and cytochrome c-mediated PARP cleavage). *Toxicol*. 2004;197(3):239–251. doi:10.1016/j.tox.2004.01.010
26. Xie X-W. Liquiritigenin attenuates cardiac injury induced by high fructose-feeding through fibrosis and inflammation suppression. *Biomed Pharmacother*. 2017;86:694–704. doi:10.1016/j.biopha.2016.12.066
27. GU J, LI H, QIN K, et al. Determination of the equilibrium solubility and apparent oil/water partition coefficients of liquiritigenin using HPLC. *Chin J Pharm Anal*. 2013;33(8):1293–1297. doi:10.16155/j.0254-1793.2013.08.016
28. Nasirideen S, Kaş HS, Öner F, Alpar R, Hincal AA. Naproxen incorporated lipid emulsions. I. Formulation and stability studies. *J Clin Pharm Ther*. 1998;23(1):57–65. doi:10.1046/j.1365-2710.1998.00139.x
29. Zhang T, Zheng Y, Peng Q, Cao X, Gong T, Zhang Z. A novel sub-micron emulsion system loaded with vincristine–oleic acid ion-pair complex with improved anticancer effect: in vitro and in vivo studies. *Int J Nanomedicine*. 2013;8:1185–1196. doi:10.2147/IJN.S41775
30. Li H, Pan T, Cui Y, et al. Improved oral bioavailability of poorly water-soluble glimepiride by utilizing microemulsion technique. *Int J Nanomedicine*. 2016;11:3777–3788. doi:10.2147/IJN.S105419
31. Rezaei A, Varshosaz J, Fesharaki M, Farhang A, Jafari SM. Improving the solubility and in vitro cytotoxicity (anticancer activity) of ferulic acid by loading it into cyclodextrin nanosponges. *Int J Nanomedicine*. 2019;14:4589–4599. doi:10.2147/IJN.S206350
32. Hu X-B, Tang T-T, Li Y-J, et al. Phospholipid complex based nanoemulsion system for oral insulin delivery: preparation, in vitro, and in vivo evaluations. *Int J Nanomedicine*. 2019;14:3055–3067. doi:10.2147/IJN.S198108
33. Zhao J, Yuan Q, Cai W, Sun P, Ding L, Jin F. Formulation, optimization, characterization, and pharmacokinetics of progesterone intravenous lipid emulsion for traumatic brain injury therapy. *AAPS PharmSciTech*. 2017;18(5):1475–1487. doi:10.1208/s12249-016-0637-5
34. Jumaa M, Müller BW. The effect of oil components and homogenization conditions on the physicochemical properties and stability of parenteral fat emulsions. *Int J Pharm*. 1998;163(1):81–89. doi:10.1016/S0378-5173(97)00369-4
35. Lipinski CA, Lombardo F, Dominy BW, Feeney PJ. Experimental and computational approaches to estimate solubility and permeability in drug discovery and development settings. *Adv Drug Deliv Rev*. 1997;23(1):3–25. doi:10.1016/S0169-409X(96)00423-1
36. Novitzky N, Thomas V, Abrahams L, du Toit C, McDonald A. Increasing dose intensity of anthracycline antibiotics improves outcome in patients with acute myelogenous leukemia. *Am J Hematol*. 2004;76(4):319–329. doi:10.1002/ajh.20120
37. Octavia Y, Tocchetti CG, Gabrielson KL, Janssens S, Crijns HJ, Moens AL. Doxorubicin-induced cardiomyopathy: from molecular mechanisms to therapeutic strategies. *J Mol Cell Cardiol*. 2012;52(6):1213–1225. doi:10.1016/j.yjmcc.2012.03.006
38. Granados-Principal S, El-azem N, Pamplona R, et al. Hydroxytyrosol ameliorates oxidative stress and mitochondrial dysfunction in doxorubicin-induced cardiotoxicity in rats with breast cancer. *Biochem Pharmacol*. 2014;90(1):25–33. doi:10.1016/j.bcp.2014.04.001
39. Lin M, Yin M. Preventive effects of ellagic acid against doxorubicin-induced cardio-toxicity in mice. *Cardiovasc Toxicol*. 2013;13(3):185–193. doi:10.1007/s12012-013-9197-z
40. Maejima Y, Kuroda J, Matsushima S, Ago T, Sadoshima J. Regulation of myocardial growth and death by NADPH oxidase. *J Mol Cell Cardiol*. 2011;50(3):408–416. doi:10.1016/j.yjmcc.2010.12.018
41. Konorev EA, Kotamraju S, Zhao H, Kalivendi S, Joseph J, Kalyanaraman B. Paradoxical effects of metalloporphyrins on doxorubicin-induced apoptosis: scavenging of reactive oxygen species versus induction of heme oxygenase-1. *Free Radic Biol Med*. 2002;33(7):988–997. doi:10.1016/S0891-5849(02)00989-9
42. Zhang Y-W, Shi J, Li Y-J, Wei L. Cardiomyocyte death in doxorubicin-induced cardiotoxicity. *Arch Immunol Ther Exp*. 2009;57(6):435–445. doi:10.1007/s00005-009-0051-8
43. Deng S, Kruger A, Kleschyov AL, Kalinowski L, Daiber A, Wojnowski L. Gp91phox-containing NAD(P)H oxidase increases superoxide formation by doxorubicin and NADPH. *Free Radic Biol Med*. 2007;42(4):466–473. doi:10.1016/j.freeradbiomed.2006.11.013
44. Khan M, Varadharaj S, Ganesan LP, et al. C-phycoerythrin protects against ischemia-reperfusion injury of heart through involvement of p38 MAPK and ERK signaling. *Am J Physiol Heart Circ Physiol*. 2006;290(5):H2136–H2145. doi:10.1152/ajpheart.01072.2005

45. Lou H, Danelisen I, Singal PK. Involvement of mitogen-activated protein kinases in adriamycin-induced cardiomyopathy. *Am J Physiol Heart Circ Physiol.* 2005;288(4):H1925–H1930. doi:10.1152/ajpheart.01054.2004
46. Li S, Mingyan E, Yu B. Adriamycin induces myocardium apoptosis through activation of nuclear factor κ B in rat. *Mol Biol Rep.* 2008;35(4):489–494. doi:10.1007/s11033-007-9112-4
47. Wang Z-Q, Chen M-T, Zhang R, Zhang Y, Li W, Li Y-G. Docosahexaenoic acid attenuates doxorubicin-induced cytotoxicity and inflammation by suppressing NF- κ B/iNOS/NO signaling pathway activation in H9C2 cardiac cells. *J Cardiovasc Pharm.* 2016;67(4):283. doi:10.1097/FJC.0000000000000350
48. Thomas CM, Yong QC, Rosa RM, et al. Cardiac-specific suppression of NF- κ B signaling prevents diabetic cardiomyopathy via inhibition of the renin-angiotensin system. *Am J Physiol Heart Circ Physiol.* 2014;307(7):H1036–H1045. doi:10.1152/ajpheart.00340.2014
49. El-Agamy DS, El-Harbi KM, Khoshhal S, et al. Pristimerin protects against doxorubicin-induced cardiotoxicity and fibrosis through modulation of Nrf2 and MAPK/NF- κ B signaling pathways. *Cancer Manag Res.* 2018;11:47–61. doi:10.2147/CMAR.S186696
50. Gu J, Hu W, Song Z, Chen Y, Zhang D, Wang C. Resveratrol-induced autophagy promotes survival and attenuates doxorubicin-induced cardiotoxicity. *Int Immunopharmacol.* 2016;32:1–7. doi:10.1016/j.intimp.2016.01.002
51. Katamura M. Curcumin attenuates doxorubicin-induced cardiotoxicity by inducing autophagy via the regulation of JNK phosphorylation. *J Clin Exp Cardiol.* 2014;05(09). doi:10.4172/2155-9880.1000337
52. Smith CC, Guévremont D, Williams JM, Napper RM. Apoptotic cell death and temporal expression of apoptotic proteins Bcl-2 and Bax in the hippocampus, following binge ethanol in the neonatal rat model. *Alcohol Clin Exp Res.* 2015;39(1):36–44. doi:10.1111/acer.12606
53. Childs AC, Phaneuf SL, Dirks AJ, Phillips T, Leeuwenburgh C. Doxorubicin treatment in vivo causes cytochrome c release and cardiomyocyte apoptosis, as well as increased mitochondrial efficiency, superoxide dismutase activity, and Bcl-2: bax ratio. *Cancer Res.* 2002;62(16):4592–4598.
54. Li W, Lin X, Yang Z, et al. A bufadienolide-loaded submicron emulsion for oral administration: stability, antitumor efficacy and toxicity. *Int J Pharm.* 2015;479(1):52–62. doi:10.1016/j.ijpharm.2014.12.054
55. Weyenberg W, Filev P, Van den Plas D, et al. Cytotoxicity of submicron emulsions and solid lipid nanoparticles for dermal application. *Int J Pharm.* 2007;337(1):291–298. doi:10.1016/j.ijpharm.2006.12.045

International Journal of Nanomedicine

Dovepress

Publish your work in this journal

The International Journal of Nanomedicine is an international, peer-reviewed journal focusing on the application of nanotechnology in diagnostics, therapeutics, and drug delivery systems throughout the biomedical field. This journal is indexed on PubMed Central, MedLine, CAS, SciSearch®, Current Contents®/Clinical Medicine,

Journal Citation Reports/Science Edition, EMBase, Scopus and the Elsevier Bibliographic databases. The manuscript management system is completely online and includes a very quick and fair peer-review system, which is all easy to use. Visit <http://www.dovepress.com/testimonials.php> to read real quotes from published authors.

Submit your manuscript here: <https://www.dovepress.com/international-journal-of-nanomedicine-journal>